

Fe-based soft magnetic amorphous alloys with a wide supercooled liquid region

著者	Koshiba H., Inoue A., Makino A.
journal or publication title	Journal of Applied Physics
volume	85
number	8
page range	5136-5138
year	1999
URL	http://hdl.handle.net/10097/52261

doi: 10.1063/1.369102

Fe-based soft magnetic amorphous alloys with a wide supercooled liquid region

H. Koshiba^{a)} and A. Inoue

Inoue Superliquid Glass Project, Exploratory Research For Advanced Technology, Japan Science and Technology Corporation, Yagiyamaminami 2-1-1, Taihaku-ku, Sendai 982-0807, Japan

A. Makino

Central Research Laboratory, Alps Electric Co. Ltd., Nagaoka 940-8572, Japan

Amorphous alloys with a wide supercooled liquid region (ΔT_x) before crystallization were formed in the $\text{Fe}_{56}\text{Co}_7\text{Ni}_7\text{Hf}_8\text{M}_2\text{B}_{20}$ ($\text{M}=\text{Nb}, \text{Ta}$) alloys by melt spinning. The ΔT_x which is a critical factor of glass-forming ability, increases to large values exceeding 90 from 82 K by the addition of 2 at. % M, and the largest ΔT_x value is larger by about 10 K than the largest value for recently reported (Fe,Co,Ni)-Zr-M-B alloys. By the addition of the M metals, magnetic properties also changed. Good soft magnetic properties were obtained for the alloys annealed for 300 s at 800 K. The saturation magnetization (I_s), coercive force (H_c), and effective permeability (μ_e) at 1 kHz are, respectively, 0.71 T, 1.0 A/m, and 16 700 for the $\text{M}=\text{Nb}$ alloy and 0.76 T, 1.0 A/m, and 15 600 for the $\text{M}=\text{Ta}$ alloy. The finding of the Fe-based amorphous alloys exhibiting simultaneously the wide supercooled liquid region before crystallization and the good soft magnetic properties seem to enable the future development of a new ferromagnetic bulk amorphous alloy. © 1999 American Institute of Physics. [S0021-8979(99)15308-8]

INTRODUCTION

It is well known that Fe-based amorphous alloys exhibit good soft magnetic properties.¹ However, these alloys have usually been prepared in a thin sheet form with a thickness below about 50 μm (Ref. 1) and in a wire form with a diameter below about 120 μm .² The small maximum thickness resulting from the low glass-forming ability for conventional Fe-based amorphous alloys has prevented the further extension of application fields as magnetic materials. Recently, the Fe-Zr-B-based bulk amorphous alloys with thickness up to 5 mm have been formed in conventional casting processes.³ These alloys consist of multicomponent systems and exhibit a glass transition, followed by a wide supercooled liquid region before crystallization.⁴⁻⁷ Furthermore, these have always satisfied the following three empirical rules^{8,9} for achievement of high glass-forming ability, i.e., (1) multicomponent alloy systems consisting of more than three elements, (2) significantly different atomic size ratios above about 12% among the main constituent elements, and (3) negative heats of mixing among their elements. Based on the three empirical rules, it has been found that a wide supercooled liquid region exceeding 80 K before crystallization is also obtained for amorphous alloys in the Fe-Co-Ni-Hf-B system.¹⁰ This article aims to present the compositional dependence of Hf or B and the influence of partial replacement of Hf by the transition metal (M) on the glass transition temperature (T_g), crystallization temperature (T_x), supercooled liquid region ($\Delta T_x = T_x - T_g$), and magnetic properties for Fe-Co-Ni-Hf-M-B amorphous alloys.

EXPERIMENTAL PROCEDURE

Master ingots of Fe-Co-Ni-Hf-M-B ($\text{M}=\text{Nb}, \text{Ta}$) alloys were prepared by arc melting the mixture of pure Fe, Co, Ni, Zr and M metals and pure B crystal in an argon atmosphere. The alloy compositions represent the nominal atomic percentage of the mixtures. Rapidly solidified ribbons with a cross section of $0.02 \times 1.0 \text{ mm}^2$ were prepared by melt spinning. The crystallized structure was examined by x-ray diffractometry (XRD). Thermal stability associated with glass transition, supercooled liquid region, and crystallization was examined at a heating rate of 0.67 K/s by differential scanning calorimetry (DSC). Magnetization at room temperature was measured in a maximum applied field of 1260 kA/m with a vibrating sample magnetometer (VSM). Coercive force was measured with a I-H curve tracer. Permeability was evaluated at 1 kHz with an impedance analyzer. Saturated magnetostriction (λ_s) was measured under a field of 240 kA/m by a three-terminal capacitance method.

RESULTS AND DISCUSSION

An amorphous phase without crystallinity was formed in the composition range of more than 0% Hf and 8% B in the rapidly solidified $\text{Fe}_{86-x-y}\text{Co}_7\text{Ni}_7\text{Hf}_x\text{B}_y$. Based on DSC curves, the T_g , T_x and ΔT_x for the Fe-Co-Ni-Hf-B amorphous alloys were plotted as a function of (a) Hf and (b) B contents in Fig. 1. The glass transition is observed in the composition range above 4% Hf and 8% B, followed by a supercooled liquid region in the temperature range below T_x . The T_g and T_x increase by the replacement of Hf and B and then only T_g slightly decreases in the B concentration range above 20 at. %. The ΔT_x changes by the difference in the compositional dependence of T_g and T_x and reaches a maximum value of 82 K at the composition of

^{a)}Electronic mail: koshiba@imr.tohoku.ac.jp

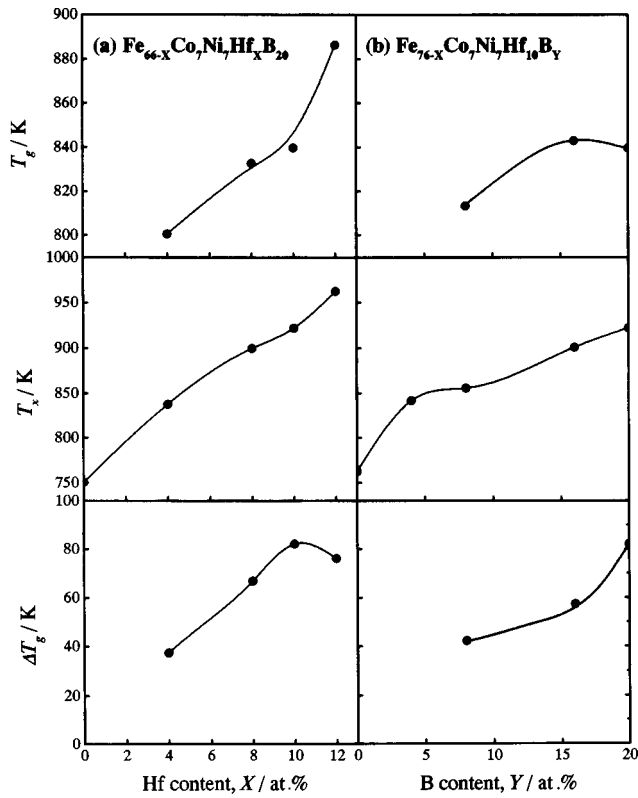


FIG. 1. Changes in the glass transition temperature (T_g), onset temperature of crystallization (T_x), and the temperature interval of supercooled liquid region ($\Delta T_x = T_x - T_g$) as a function of (a) Hf and (b) B contents for the amorphous $Fe_{86-x-y}Co_7Ni_7Hf_xB_y$ alloys.

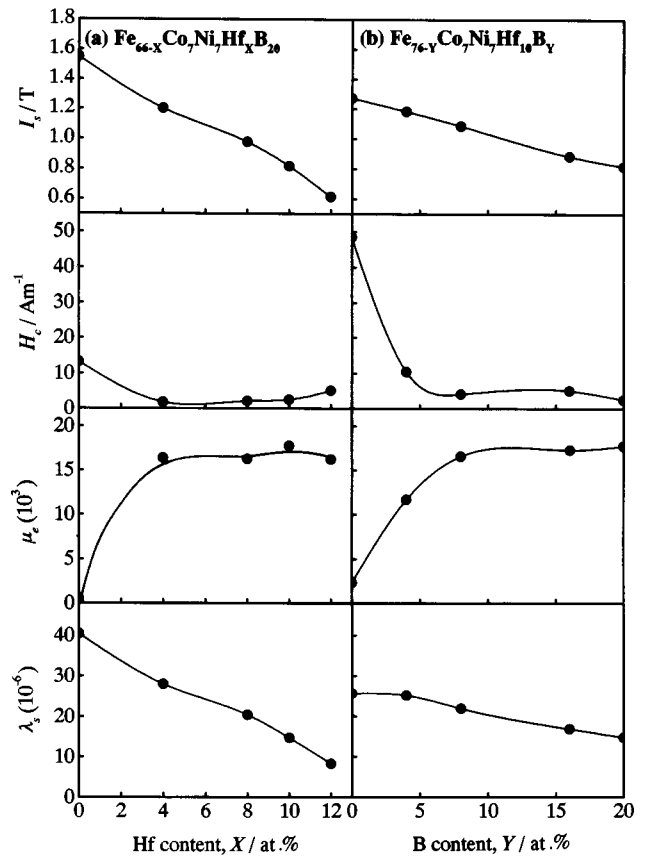


FIG. 2. Changes in saturation magnetization (I_s), coercive force (H_c), effective permeability (μ_e) at 1 kHz and saturated magnetostriction (λ_s) as a function of (a) Hf and (b) B contents for the amorphous $Fe_{86-x-y}Co_7Ni_7Hf_xB_y$ alloys in annealed states.

$Fe_{56}Co_7Ni_7Hf_{10}B_{20}$. From these results, it is clear that the replacement of Fe by Hf and B is effective for the improvement of glass-forming ability. Similarly, Fig. 2 shows the saturation magnetization (I_s), coercive force (H_c), effective permeability (μ_e) at 1 kHz, and saturated magnetostriction (λ_s) as a function of (a) Hf or (b) B content for the $Fe_{86-x-y}Co_7Ni_7Hf_xB_y$ amorphous alloys in annealed states. Here, the annealing was made at the temperature 40 K lower than T_g . As is the case for thermal stability, the magnetic properties also change by the replacement of Hf and B. It is seen that the replacement by Hf and B causes a gradual decrease in I_s and λ_s and a significant decrease in H_c in the range up to 4% Hf and 8% B. The H_c keeps a low value of about 2 A/m in the higher Hf and B concentration range. On the other hand, the μ_e significantly increases in the range up to 4% Hf and 8% B and then keeps a high value of about 17 000. The resulting, H_c and μ_e values are significantly improved and exhibit the best values of 2.5 A/m and 17 800, respectively, for the $Fe_{56}Co_7Ni_7Hf_{10}B_{20}$ alloy. It seems that I_s falls by the decrease of Fe and H_c and μ_e are improved with stabilization of the alloys. Therefore, it is said that this alloy exhibits simultaneously high glass-forming ability and good soft magnetic properties.

Secondly, based on the results of Fe-based amorphous alloys reported to date,^{11,12} we have made the partial replacement of Hf by 2 at. % Nb or Ta to improve the glass-forming ability of the above-mentioned $Fe_{56}Co_7Ni_7Hf_{10}B_{20}$ alloy. It is clear that the $Fe_{56}Co_7Ni_7Hf_8M_2B_{20}$ (M=Nb or Ta) alloys are

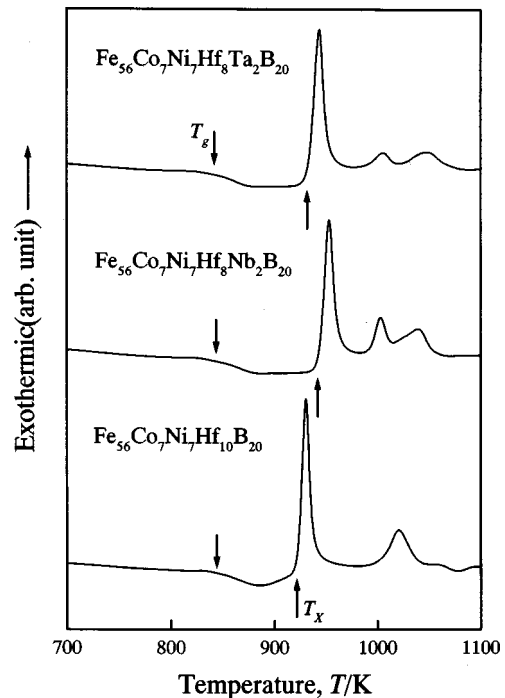


FIG. 3. DSC curves of the amorphous $Fe_{56}Co_7Ni_7Hf_{10}B_{20}$, $Fe_{56}Co_7Ni_7Hf_8Nb_2B_{20}$, and $Fe_{56}Co_7Ni_7Hf_8Ta_2B_{20}$ alloys.

TABLE I. Saturation magnetization I_s , coercive force H_c , effective permeability at 1 kHz (μ_e) and saturated magnetostriction λ_s for the $\text{Fe}_{56}\text{Co}_7\text{Ni}_7\text{Hf}_{10}\text{B}_{20}$, $\text{Fe}_{56}\text{Co}_7\text{Ni}_7\text{Hf}_8\text{Nb}_2\text{B}_{20}$, and $\text{Fe}_{56}\text{Co}_7\text{Ni}_7\text{Hf}_8\text{Ta}_2\text{B}_{20}$ amorphous alloys annealed for 300 s at 800 K.

	I_s (T)	H_c (A/m)	μ_e (1 kHz)	$\lambda_s(10^{-6})$
$\text{Fe}_{56}\text{Co}_7\text{Ni}_7\text{Hf}_{10}\text{B}_{20}$	0.82	2.5	17 800	14
$\text{Fe}_{56}\text{Co}_7\text{Ni}_7\text{Hf}_8\text{Ta}_2\text{B}_{20}$	0.76	1.0	15 600	12
$\text{Fe}_{56}\text{Co}_7\text{Ni}_7\text{Hf}_8\text{Nb}_2\text{B}_{20}$	0.71	1.0	16 700	10

composed of an amorphous phase without crystallinity from XRD results. Figure 3 shows DSC curves of the $\text{Fe}_{56}\text{Co}_7\text{Ni}_7\text{Hf}_8\text{M}_2\text{B}_{20}$ ($M=\text{Hf, Nb, or Ta}$) amorphous alloys. One can see a distinct glass transition, followed by a wide supercooled liquid region in the temperature range before crystallization for these alloys. The ΔT_x increases to large values exceeding 90 K by the addition of 2 at. % M, being larger by about 10 K than the largest value for recently reported Fe-Co-Ni-Zr-M-B ($M=\text{Nb or Ta}$) alloys.^{11,12} Table I summarizes I_s , H_c , μ_e at 1 kHz and λ_s for the $\text{Fe}_{56}\text{Co}_7\text{Ni}_7\text{Hf}_8\text{M}_2\text{B}_{20}$ amorphous alloys subjected to annealing for 300 s at 800 K just below T_x . It is seen that the replacement of Hf by M elements causes a decrease of I_s . The I_s decreases by 0.06 to 0.11 T only by the addition of 2% M. The μ_e values also slightly decrease, but nevertheless keep high values of 15 500–16 500. Additionally, the H_c also exhibits a low value of 1.0 A/m. From the compositional dependence of the thermal stability of the supercooled liquid and the magnetic properties, it is concluded that the $\text{Fe}_{56}\text{Co}_7\text{Ni}_7\text{Hf}_8\text{M}_2\text{B}_{20}$ ($M=\text{Nb or Ta}$) amorphous alloys have the useful characteristics of high glass-forming ability and good soft magnetic properties.

Finally, the reason for the large ΔT_x for the Fe-based amorphous alloys is discussed in the framework of the three empirical rules for the achievement of high glass-forming ability. The base composition is the Fe-Hf-B ternary system which satisfies the three empirical rules. The addition of Nb or Ta is effective for the increase in the degree of satisfaction of the empirical rules. That is, the addition of these elements causes the more sequential change in the atomic size on the order of $\text{Hf} \gg \text{Nb (Ta)} > \text{Fe, Co} \gg \text{B}$ as well as the generation of new atomic pairs with various negative heats of mixing. In the supercooled liquid in which the three empirical rules are

satisfied at a high level, the topological and chemical short-range orderings are enhanced, leading to the formation of a highly dense random packed structure with low atomic diffusivity. Therefore, the diffusivity of the constituent elements is suppressed and the liquid/solid interfacial energy is increased. Even in the supercooled liquid structure, long-range atomic rearrangements are required for precipitation of the crystalline phases. However, the atomic rearrangements are difficult in the specialized liquid with low diffusivity. The difficulty seems to be the reason for the appearance of the glass transition and supercooled liquid region before crystallization.

CONCLUSIONS

The glass transition and subsequent supercooled liquid region were observed in the temperature range before crystallization for all the $\text{Fe}_{56}\text{Co}_7\text{Ni}_7\text{Hf}_8\text{M}_2\text{B}_{20}$ alloys. The ΔT_x increases by the addition of 2% M and reaches a maximum ΔT_x of 98 K for the 2% Nb or Ta alloys. The ΔT_x is the largest among Fe-based amorphous alloys reported here. Furthermore, these alloys annealed for 300 s at 800 K exhibit good soft magnetic properties, i.e., H_c of 1.0 A/m and μ_e of 15 000–17 000 at 1 kHz. The finding of the new amorphous alloys with the two characteristics is important for the future development of bulk amorphous alloys in the application of soft magnetic materials.

¹ *Materials Science of Amorphous Metals*, edited by T. Masumoto (Ohmu, Tokyo, 1982).

² M. Hagiwara, A. Inoue, and T. Masumoto, *Metall. Trans. A* **13A**, 373 (1982).

³ A. Inoue, T. Zhang, and A. Takeuchi, *Appl. Phys. Lett.* **71**, 464 (1997).

⁴ A. Inoue, A. Takeuchi, T. Zhang, A. Murakami, and A. Makino, *IEEE Trans. Magn.* **32**, 4866 (1996).

⁵ A. Inoue, K. Kita, T. Zhang, and T. Masumoto, *Mater. Trans., JIM* **30**, 722 (1989).

⁶ A. Peker and W. L. Johnson, *Appl. Phys. Lett.* **63**, 2342 (1993).

⁷ A. Inoue, N. Nishiyama, and T. Matsuda, *Mater. Trans., JIM* **37**, 181 (1996).

⁸ A. Inoue, T. Zhang, and T. Masumoto, *J. Non-Cryst. Solids* **156–158**, 473 (1993).

⁹ A. Inoue, *Mater. Trans., JIM* **36**, 866 (1995).

¹⁰ H. Koshiba, A. Inoue, and A. Makino, *The Third Pacific Rim International Conference on Advanced Materials and Processing* **1**, 1023 (1998).

¹¹ A. Inoue, H. Koshiba, T. Zhang, and A. Makino, *Mater. Trans., JIM* **38**, 577 (1997).

¹² A. Inoue, H. Koshiba, T. Zhang, and A. Makino, *J. Appl. Phys.* **83**, 1967 (1997).